RSC Advances

PAPER

View Article Online
View Journal | View Issue

Cite this: *RSC Adv.*, 2017, **7**, 33701

PU/PMMA composites synthesized by reaction-induced phase separation: a general approach to achieve a shape memory effect†

Yufen Zhang,‡[a] Weiwei Li,‡[a] Ronglan Wu*[a] and Wei Wang *[ab]

Received 8th May 2017
Accepted 24th June 2017

DOI: 10.1039/c7ra05206e

rsc.li/rsc-advances

We report a study on the triple-shape memory polymer composition of polyurethane/polymethyl methacrylate (PU/PMMA) synthesized using reaction-induced phase separation. Microscopic phase separation, which forms sea-island structures, enhances the shape memory effect, and phase separation can be achieved by changing the volume ratio of the two components in the polymer composites. In this study, we used the same method and synthesized 5 composites with different volume ratios of PU/PMMA. The composites with a PU/PMMA ratio of 2 : 1 exhibited triple-shape memory effect. The PU/PMMA composites were characterized by X-ray photoelectron spectroscopy (XPS), Fourier transform infrared spectroscopy (FTIR), differential scanning calorimetry (DSC), scanning electron microscopy (SEM) and dynamic mechanical analysis (DMA). Based on the studies, we propose that reaction-induced phase separation can be used as a general approach to achieve the shape memory effect.

1 Introduction

Shape memory polymers (SMPs) are smart materials that respond to external stimuli, such as light, heat, pH, *etc.*[1–4] In a SMP, one or more temporary shapes, each determined by the network elasticity, can be programmed in the materials.[5] By providing a stimulus, the programmed stress drives the polymer shape to deform and revert to its original shape.[6] Due to their unique properties, SMPs have found potential applications in medicine, biotechnology, biosensors, *etc.*[7–9]

Polymers are generally soft and deformable above the glass transition temperature (T_g) or melting temperature (T_m). Therefore, it has been argued that the thermally induced dual-shape memory effect (SME) is an intrinsic property for polymers, due to the existence of T_g and T_m.[10] However, in most polymers and polymer composites, external stress can hardly be stored above the deformation temperature (T_d), meaning that the deformation is often permanent. The deformation of SMPs at temperatures above T_d is often not permanent, which is due to the molecular construction of SMPs.[11] Based on many studies on the synthesis of SMPs, a general theory has discerned that two elements, netpoints (fixed phase) and molecular switches (reversible phase), are required to construct a SMP.[12] As an example, these two elements are realized as soft segments and hard segments in polyurethane (PU), a model thermally-induced SMP.[13] In PU, the soft segments further soften above T_d and provide a feature of deformation; meanwhile, reversible stress can be programmed into the hard segments by reducing the temperature to below T_d.[14,15]

This underlying principle can be used to construct SMPs by blending two or more polymers with distinct reversible phase transitions.[16] A temporary shape can be programmed into a polymer composite when one component is soft and the other remains stiff. In this case, the soft component acts as the reversible phase; the stiff component acts as the fixed phase.[17] This analysis for polymer composites indicates that, in order to construct a thermally induced shape memory polymer composite (SMPC), segregative phase separation must occur because otherwise there will be only one phase transition temperature, and above this temperature, both polymers become deformable.[18] The reaction-induced phase separation enables a polymer composite to have two or more transition temperatures.[19] Thus, it could be employed as a novel and effective method to construct SMPCs with multiple shape memory effects. Tao Xie *et al.* prepared bilayer epoxy samples with triple-shape memory effects (TSMEs) by blending two epoxy dual-shape memory polymers with two well-separated glass transition temperatures that acted as the deformation temperatures.[20] Amir H. Torbati *et al.* prepared two types of triple-shape memory composite (TSMC) using reaction-induced phase transition. The two types of TSMC, polypropylene glycol–epoxy/poly(ε-caprolactone) (PPG–EP/PCL) and polyethylene oxide–epoxy/poly(ε-caprolactone) (PEO–EP/PCL), both possessed two obvious transition temperatures that enabled

[a]*Key Laboratory of Oil and Gas Fine Chemicals, College of Chemistry and Chemical Engineering, Urumqi 830046, China. E-mail: wuronglan@163.com*

[b]*Department of Chemistry and Centre for Pharmacy, University of Bergen, Bergen 5007, Norway. E-mail: wei.wang@uib.no; wangwei@iccas.ac.cn*

† Electronic supplementary information (ESI) available: The results of XPS, DSC and static force are presented. See DOI: 10.1039/c7ra05206e

‡ These two authors contributed equally.

them to memorize two temporary shapes.[21] So far, a few reports have paid attention to constructing shape memory polyurethane (SMPU) with a triple-shape memory effect using reaction-induced phase separation. In our previous study, we reported the synthesis of polymer composites composed of dual-shape memory polyurethane and poly(methacrylic acid) (PMAA) using reaction-induced phase separation.[22] Because of the broad phase transition and multiphase polymers, the composite with a ratio of PU/PMAA = 3 : 1 exhibited a triple-shape memory effect. Therefore, using reaction-induced phase separation, dual-shape memory polyurethane (DSMPU) could well evolve into triple-shape memory polyurethane (TSMPU). However, the relationship between the degree of phase separation (DPS) and SME requires further investigation.

In a segregative system, phase separation can be realized by the reduction of the mixing entropy, especially at a high degree of polymerization.[23,24] In general, the monomers before polymerization are often miscible. The evolution from a miscible mixture to a phase-separated composite suggests that phase separation and polymerization occur simultaneously during the reaction, and phase demixing competes with chemical-reaction-induced phase mixing. This competition between the two processes may lead to extremely different consequences: a complete phase separation or an interpenetration network.[25] The occurrence of phase separation depends on two parameters: χ_1 and χ_{1c}.[26] Here, χ_1 is the Flory–Huggins interaction parameter. For a system containing two components (a and b), χ_1 can be defined by the equation $\chi_1 = \left(\frac{M_a\phi_a}{\rho_a} - \frac{M_b\phi_b}{\rho_b}\right)\frac{(\delta_a - \delta_b)^2}{RT}$. Here, δ, M, ϕ and ρ represent the solubility parameters, molar masses, volume fractions, and densities of the two components. R and T have their usual physical meanings. The other critical factor, χ_{1c}, which affects the phase separation, is expressed as $\chi_{1c} = \frac{1}{2}\left(\frac{1}{\sqrt{x_a}} + \frac{1}{\sqrt{x_b}}\right)^2$, where x_a and x_b stand for the degrees of polymerization of a and b, respectively. When $\chi_{1c} < \chi_1$, phase separation will be observed. As the expression of χ_1 shows, for a system with two polymers, the value of χ_1 can be adjusted by the volume ratio of the two polymers. Zhi Wang *et al.* prepared a sea-island structure, a bicontinuous structure, and homogeneous products by changing the content of A-aniline benzoxazine (BA-a) and *N*,*N*′-(2,2,4-trimethylhexane-1,6-diyl)bis(maleimide) (TBMI).[25] Similarly, Xiaodan Li *et al.* synthesized C-BOZ/BADCy blends with sea-island phase separations by changing the ratio of the two components.[26]

In our previous study, we found that phase separation easily occurs between montmorillonite–polymethyl methacrylate (MMT–PMMA) and SMPU by simply blending their solutions.[27] Therefore, we surmised that the polymerization of methyl methacrylate in a solution of SMPU could result in phase separation between PMMA and SMPU; meanwhile, the mixture of PMMA and DSMPU showed a triple-shape memory effect. In this work, the shape memory polyurethane/polymethyl methacrylate composite (SMPU/PMMA) with TSME was prepared using a novel and effective method of reaction-induced phase separation. We adjusted and controlled the phase separation degree of the polymer composites by changing the ratio between PU and PMMA. The relationship between DPS and SME of SMPU/PMMA was investigated. The DPS increased with the volume fraction of PMMA. The SME was homoplastically enhanced by an increase in phase-separation.

2 Materials and methods

2.1 Materials

Polytetramethylene ether glycol (PTMG, molecular weight 1000 g mol^{-1}) was purchased from Hengtai Chemicals (Jining, China). 1,4-Butane-diol (BDO, > 98%) was purchased from Aladdin Corp. (Shanghai, China). *N*,*N*′-Dimethylformamide (DMF, >98%) and methyl methacrylate (MMA, >98%) were purchased from Fucheng Chemical (Tianjin, China). *N*,*N*′-Methylene bisacrylamide (BIS, >98%) was provided by Tianjin Chemical Corp. (Tianjin, China); 2,2′-azobis(1-methylpropionitrile) (AIBN) was purchased from Shanfu Chemical (Shanghai, China); 2,4-tolylene diisocyanate (TDI) was purchased from Damao Chemical Corp. (Tianjin, China). The dehydration of DMF was carried out with 4 Å molecular sieves, and then it was distilled before use. Milli-Q water with a resistivity of 18 MΩ cm was used in all experiments.

2.2 Synthesis of PTMG–polyurethane

The reaction route is presented in Fig. 1. PTMG (4.017 g) was added to a three-neck flask and warmed to 50 °C. With mechanical stirring, the sample melted after 15 minutes. TDI (6.303 g) was then mixed with the melted PTMG, and the mixture was warmed to 70 °C to conduct the reaction. The reaction was kept at 70 °C for 2 hours to yield a prepolymer. The mixture was then cooled to 60 °C, and BDO (3.154 g) and DMF (20 mL) were sequentially added. The mixture was kept at 60 °C for another 2 hours, and it then yielded a viscous liquid with a pale yellow color. This liquid was cast into a thin film and dried at 120 °C for 24 hours.

2.3 Synthesis of the PU/PMMA composites

A stream of nitrogen was flowed into the prepolymer for 15 minutes. MMA, BIS and AIBN were mixed with the prepolymer to conduct polymerization. The amounts of the reactants are shown in Table 1. Four composites were synthesized with changing weight ratios of PU and MMA. Polymerization was conducted for 2 hours at 70 °C. This yielded a viscous liquid with a pale yellow color, which was then cast into a thin film.

2.4 Characterization of PU/PMMA composites

X-ray photoelectron spectroscopy (XPS) measurements were carried out on an ESCALAB 250Xi Microprobe (ThermoFisher Scientific, USA). Monochromatised X-rays (1486.6 eV) were generated by Al Kα. High resolution spectra were recorded at 15 eV pass energy using the binding energy of C 1s (284.6 eV) as a reference. The spectra were analysed using the Gaussian–Lorentzian method with built-in software.

Fourier transform infrared spectra (FTIR) were carried out on an IR Prestige-21 (Shimadzu, Japan). The dried specimens

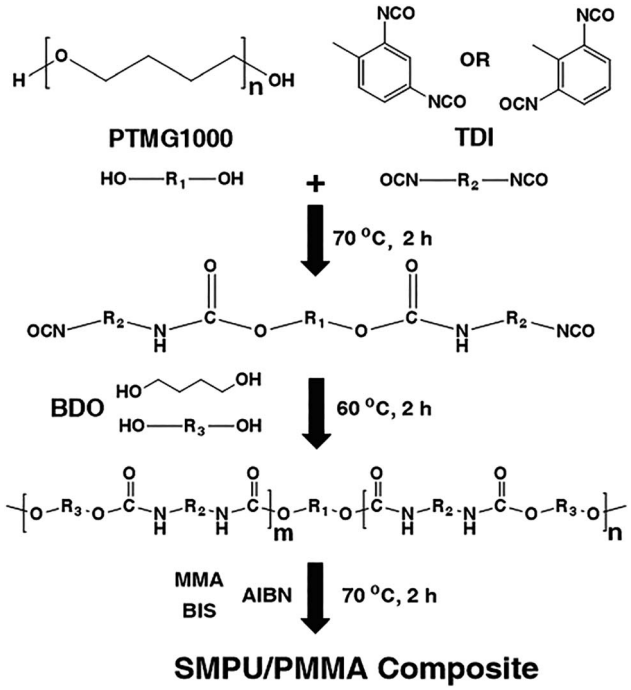

Fig. 1 The reaction route to synthesize the PU/PMMA composites.

Table 1 The weight of the reactants for each composite

PU : MMA	PU (g)	MMA (g)	AIBN (g)	BIS (g)
2 : 1	5.030	2.561	0.0510	0.0515
3 : 1	6.193	2.063	0.0417	0.0416
4 : 1	7.102	1.701	0.0342	0.0339
5 : 1	6.565	1.324	0.0260	0.0264

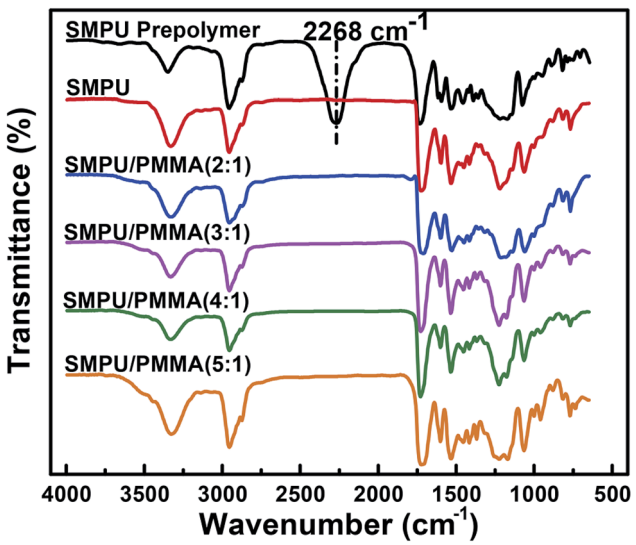

Fig. 2 FTIR spectra of the prepolymer and the PU/PMMA composites.

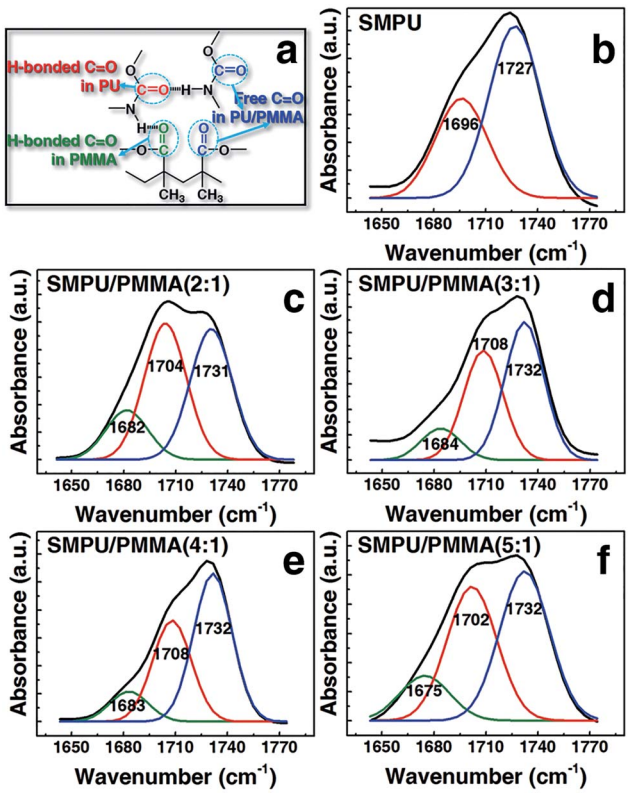

Fig. 3 (a) The three types of carbonyl group in the composites including the free carbonyl groups and the two types of hydrogen-bonded carbonyl groups. The absorption band of C=O is analyzed for (b) pure PU and the composites with different ratios of PU/PMMA in a wavenumber range of 1640–1780 cm^{-1}. The stretching vibration appears at 1730 cm^{-1} for free C=O, which shifts to 1700 cm^{-1} due to self-association and to 1680 cm^{-1} due to PU/PMMA association. The ratios of PU/PMMA are (c) 2 : 1, (d) 3 : 1, (e) 4 : 1, and (f) 5 : 1.

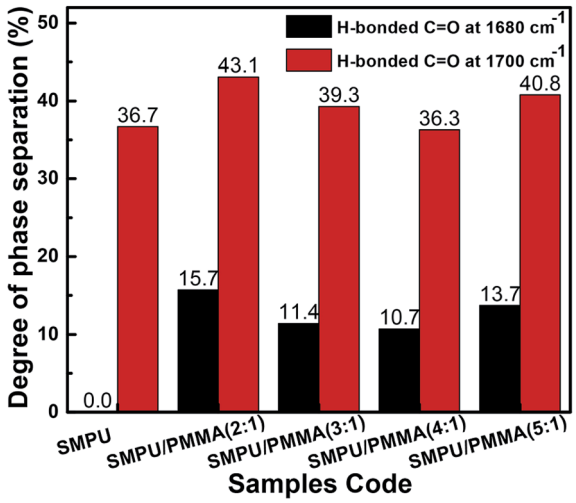

Fig. 4 The degree of phase separation is presented as a function of the ratio of PU/PMMA in the composite.

were directly used to determine the absorption in a wavenumber range of 400–4000 cm^{-1}.

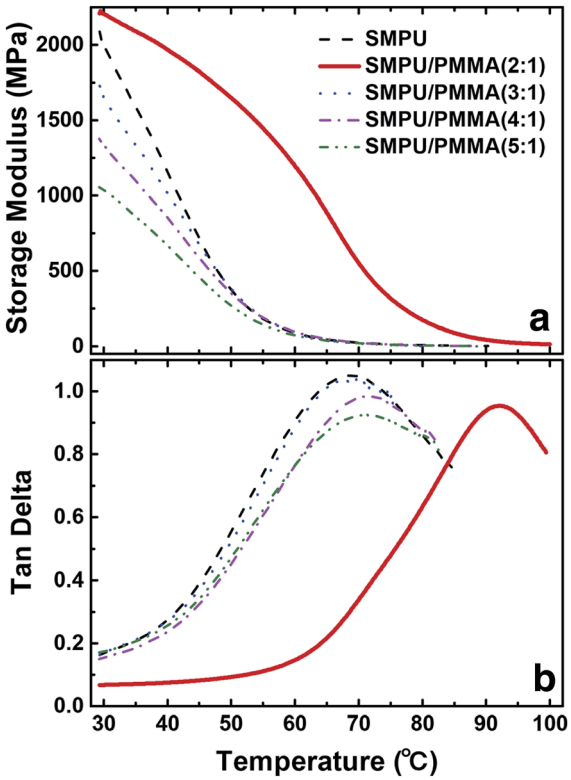

Fig. 5 DMA scans of the PU and PU/PMMA composites for (a) the storage modulus and (b) the tan δ *versus* temperature.

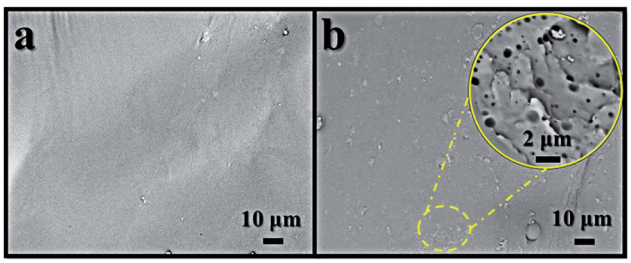

Fig. 6 SEM images of (a) PU and (b) PU/PMMA with a weight ratio of 2 : 1.

Differential scanning calorimetry (DSC) was carried out on a DSC Q2000 (TA instruments, USA). Prior to each measurement, a standard protocol was conducted to eliminate any unknown thermal history. The measurements were repeated in a temperature range of −50 to 200 °C with a rate of 10 °C min^{-1}. Nitrogen was used as the purge gas with a flow rate of 50 mL min^{-1}.

The images from scanning electron microscopy (SEM) were captured by a TM 3030 (Hitachi, Japan). The samples were prepared by following a standard protocol, and one sample was immersed in liquid nitrogen. Brittle rupture was conducted to obtain a fresh surface of this sample, and then the surface was coated with gold particles.

Dynamic mechanical analysis (DMA) was carried out on a DMA Q800 (TA instruments, USA). A specimen was cut into a cuboid with a size of 20 mm × 6.3 mm, and then the specimen was placed under tension between a fixed and moveable clamp, and a multi-frequency mode was used to operate the specimen. The measurements were conducted in a temperature range of 25 °C to 120 °C with an increase rate of 3 °C min^{-1}.

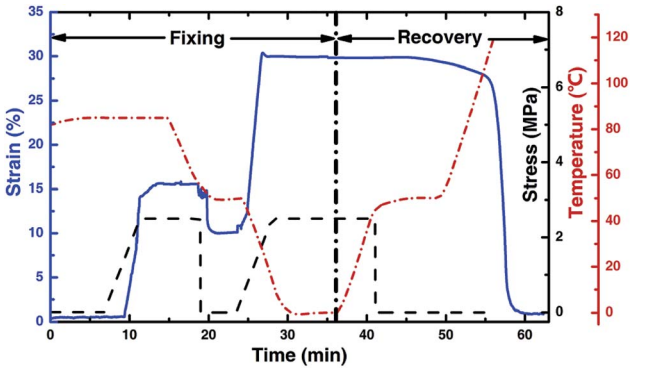

Fig. 7 The triple-shape memory behaviors recorded by DMA. The fix ratios, R_f(0−I) and R_f(I−II), are 76% and 89%, respectively; the recovery ratios, R_r(II−I) and R_r(I−0), are 79% and 93%, respectively.

The measurement of the shrinkage force was also carried out using the DMA Q800. The cuboid specimens were used with a size of 20 mm × 6.3 mm. The length of the specimen was stretched to its double at 80 °C, and then the length was fixed at 0 °C. The isostrain mode was used to operate the specimen at a constant stain of 0.01% within a temperature ramp from 25 °C to 120 °C.

The shape memory experiments were conducted on the DMA Q800. The size of the specimen here is 20 mm × 6 mm. The specimen was warmed to 60 °C for 5 minutes to be softened. The specimen was then lengthened to 40 mm (L_1). The shape was fixed at 0 °C for 5 minutes, and the length of the specimen was recorded as L_1. The specimen was then warmed, again to 60 °C, until the length did not change, and the recovered length was recorded as L_2. The same procedure was repeated four times on each specimen. The shape fixing rate (R_f) and recovery rate (R_r) were calculated based on the following equations.

$$R_f = \frac{L_1 - L_0}{L_0} \quad (1)$$

$$R_r = \frac{L_1 - L_2}{L_1 - L_0} \quad (2)$$

3 Results and discussion

3.1 FTIR and degree of phase separation

FTIR spectra of the prepolymer and PU/PMMA are presented in Fig. 2. The absorbances at 3322 cm^{-1} and 1533 cm^{-1} for the prepolymer are attributed to the stretching and bending vibrations of N–H, respectively. The characteristic absorbance for the prepolymer is the absorption band at 2268 cm^{-1}, as indicated in Fig. 2 by the dotted line, which is attributed to N=C=O. This band substantially reduced after the PU/PMMA composites

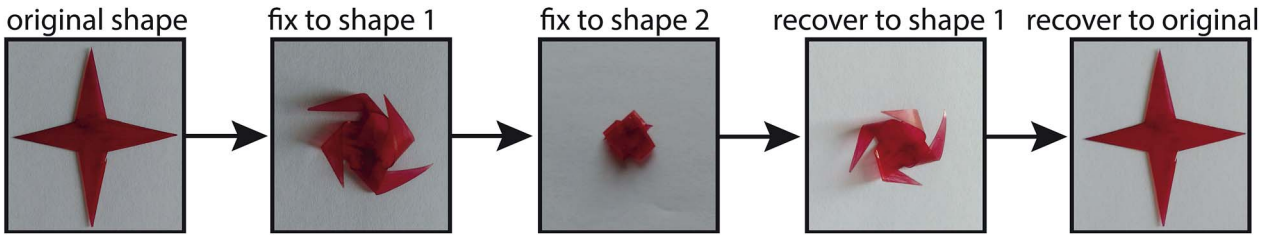

Fig. 8 One cycle of the triple-shape memory effect. The temporary shapes 1 and 2 are fixed at 50 °C and 0 °C, respectively; shape 1 and the original shape are recovered at 50 °C and 80 °C, respectively.

formed. The characteristic absorbance of C=O in PU appears at 1727 cm^{-1}. After the synthesis of PU, the stretching vibrations of C=O appear as a broad peak between 1770 cm^{-1} to 1650 cm^{-1} because the C=O in PMMA forms a hydrogen bond with the N–H groups in PU.[28] The stretching vibration of N–H (ν_{N-H}) is also affected after forming the composition with PMMA, which appears at around 3358 cm^{-1} and the intensity of the band changes with the ratio of PU/PMMA. As hydrogen bonding in the composition is crucial for the shape memory effect, we investigate the influence of the hydrogen bond on the phase separation in the composites, and further on the shape memory effect.

The hydrogen bonding in the PU/PMMA composites is manifested in the IR spectra of the three functional groups: N–H (3500–3200 cm^{-1}), C=O (1800–1600 cm^{-1}), and C–O–C (1200–1000 cm^{-1}). Within the three functional groups, N–H provides the proton; C=O and C–O–C provide the lone-pair electron. Therefore, two types of hydrogen bond, N–H···O–C and N–H···O=C, could be formed in the composites.[29] As to the later one, N–H···O=C, two types of carbonyl group are involved, one in the ester group of PMMA and the other in the carbamide group of PU, as depicted in Fig. 3a. Hence, the main intermolecular interactions in the composites are composed of two associations, the urethane groups with themselves (self-association) and with the ester group (PU/PMMA-association). As depicted in Fig. 3a, a third type of carbonyl group exists, in which the carbonyl moieties are not hydrogen-bonded to other urethane groups, namely (truly) free carbonyl groups.

The intensity of the three functional groups is dependent on the molar ratio of the soft and hard segments of PU, and the ratio of PU/PMMA. Since the molar ratio of the soft and hard segments of PU is fixed in the synthesis, only the ratio of PU/PMMA affects the intensity. As the stretching vibration of carbonyl forms hydrogen bonds with N–H, $\nu_{C=O}$ manifests as a combination of the superimposed peaks in a wavenumber range of 1650–1770 cm^{-1}, depicted in Fig. 3b for pure PU. Both the vibrations of free carbonyl groups and self-associated carbonyl groups take place in this wavenumber range. As shown in Fig. 3b, the two attributions, 1730 cm^{-1} and 1700 cm^{-1}, can be assigned to the free carbonyl groups and hydrogen-bonded carbonyl groups.

In the composites, due to the presence of PU/PMMA association, a deflection appears at a low wavenumber around 1680 cm^{-1}, which is attributed to the PU/PMMA-associated carbonyl groups. The hydrogen bond of N–H···O=C is mostly formed in the hard segments, and free carbonyl groups exist in the soft segments; therefore, the degree of phase separation in the composites could be related to the relative intensity of these two types of C=O in the FTIR spectra.[30] Quantitatively, the degree of phase separation (DPS) can be defined by the ratio of the area of $\nu_{C=O}$ that forms hydrogen-bonds to the overall intensity of carbonyl groups, and written as follows,

$$\mathrm{DPS} = \frac{A_{h,i}}{\sum_i A_{h,i} + A_f}$$

where $A_{h,i}$ represents the peak area of the hydrogen-bonded carbonyl groups, and A_f represents the peak area of the free carbonyl groups.[31] In our study, an absorption band in a wavenumber range of 1640–1780 cm^{-1} is analyzed quantitatively, as shown in Fig. 3. The DPS caused by each of the hydrogen bonds was calculated and is presented in Fig. 4. The result clearly shows that DPS increases with the relative mass of PMMA in the composite. As shown in Fig. 4, a dramatic change occurs at a mass ratio of PU/PMMA of 2 : 1, the degree of phase separation reaches 43.1% and 15.7% for H-bonded C=O at 1680 and 1700 cm^{-1}, respectively. Fig. 4 also shows that the DPS for the

Table 2 The shape fix ratios and recovery ratios of four cycles of the shape memory tests for the PU and PU/PMMA composites

	1st		2nd		3rd		4th	
Sample no.	R_f (%)	R_r (%)	R_f (%)	R_r (%)	R_f (%)	R_r (%)	R_f (%)	R_r (%)
PU	100	88.2	100	78.9	100	75	96	71.4
PU/PMMA (5 : 1)	100	89.3	100	75	93.8	71.4	90.2	71.4
PU/PMMA (4 : 1)	100	90.2	100	78.9	96.7	75	96.7	71.4
PU/PMMA (3 : 1)	100	93	100	83.7	100	75	96.3	71.8
PU/PMMA (2 : 1)	100	93.2	100	88.2	100	82	96.3	78

5 : 1 composites is on a level of 40.8% to 13.7% for H-bonded C=O at 1680 and 1700 cm^{-1}, respectively. They are slightly lower than the values for PU/PMMA at 2 : 1. In spite of the 5 : 1 composition, a monotonic increase of DPS was observed with an increase of the PMMA ratio in the composition, which is induced by polymerization-induced phase separation. Due to the dramatic change in the state of phase separation, the materials were further investigated for their mechanical properties in response to temperature.

3.2 Mechanical properties

Fig. 5 shows the dynamic mechanical analysis of all composites. The storage modulus and tan δ are presented as a function of temperature. A distinct difference was found between the composite with a weight ratio of 2 : 1 and the rest of the composites. The storage modulus decreases at a low temperature after adding PMMA in the composites. For the three composites with weight ratios of 3 : 1, 4 : 1 and 5 : 1, the storage moduli are all lower than pure PU. However, the storage modulus increases with the weight ratio of PMMA in the composites. The storage modulus for the 2 : 1 composite is dramatically increased, and a two-stage decay is observed. One is from 30 °C to 60 °C (slow decay); the other from 60 °C to 90 °C (fast decay). This indicates that segregation has occurred in the composite, where the slow decay is attributed to PU and the fast decay is attributed to PMMA.

This change is also manifested on the tan δ–temperature curves where the glass transition of the composites could be read. PU shows the lowest glass transition temperature (T_g), which is 68 °C. The composites with low PMMA content also show slightly higher T_g compared to the T_g of pure PU. In the composites with low PMMA content, T_g shows independence to the PMMA content. This suggests that the blend microstructure is independent of the PMMA content in the composites. As for the composite with a weight ratio of 2 : 1, tan δ exhibits a peak value at 92 °C, which is a great discrepancy compared to pure PU and the other composites. In the tan δ–temperature curve for the 2 : 1 composite, only one T_g is observed. By the addition of PMMA, the composites exhibit a much broader region of transition, as shown in the results of DSC in Fig. S2.† With the increase of PMMA in the composites, the endothermic peak extends the region from 20 °C to nearly 175 °C for the 2 : 1 composite. This extension in terms of the transition temperature greatly affects the shape memory effect of the materials. As it was reported earlier, the broadened transition-temperature region may benefit the shape memory effect for a single-component material.[32] However, we do not think it is the essential reason for improving the shape memory of multiple-component materials. As we compare the composites with weight ratios of 3 : 1 and 2 : 1, both of them have a wide range of transition temperatures; while, based on the results from DMA, the material with a weight ratio of 3 : 1 behaves very similar to pure PU. But the storage modulus and tan δ have changed completely for the composite with a weight ratio of 2 : 1. Therefore, the microstructure was further investigated. In the next sections, we will present the microstructure and shape memory effect for the 2 : 1 composite to illustrate the effect of microstructure on the shape memory effect.

3.3 Micro-morphology studied by SEM

SEM was employed to investigate the microstructure of PU and the composites. The SEM images of both the specimens are presented in Fig. 6. As shown in Fig. 6a, the fractured surface of the PU specimen is essentially smooth in a large area, while a very rough surface is observed for composites with a weight ratio of 2 : 1, as shown in Fig. 6b. On the scale of 2 μm, a large amount of holes and beads are shown on the fractured surface. Some beads are on a scale of 1–5 μm. The structure is referred to as a sea-island structure in polymer blends. The change of the micro-structure due to the formation of beads is substantial. For polymer blends, this structure may sometimes cause a shoulder peak on tan δ–temperature curves indicating a particulate phase-separation.[33] However, in Fig. 5b, we could not identify it, so it may be covered by tan δ rising from 60 °C to 90 °C. By the comparison of Fig. 6a and b, the micro-structure of the materials has been changed by the addition of PMMA. Particulate phase-separation is observed in the SEM image (Fig. 6b), which indicates that the micro-structure change may have a decisive impact on the properties of the material. In the next section, the shape memory effect of the composite with a weight ratio of 2 : 1 is characterized. Interesting triple-shape memory properties are recorded by DMA and a macroscopic shape change.

3.4 Triple-shape memory

Pure PU exhibits dual-shape memory properties. The mechanism is due to micro-phase separation between the hard segments and soft segments. Above the deformation temperature, the hard segments will act as physical net points, and the soft segments are softened. A temperature shape can be memorized by installing stress in the material. Micro-phase separation and the freezing mechanism are essential for this type of shape memory polymer. Here, we have observed particulate phase separation after the addition of PMMA with a weight ratio of 2 : 1. Therefore, a triple-shape memory effect may be expected. Based on the results of DMA and DSC, 50 °C and 80 °C were chosen as the temperatures to test the triple-shape memory effect for the composite. The DMA results and macroscopic shape change are recorded and presented in Fig. 7 and 8.

As shown in Fig. 7, the temperature was first increased to 80 °C. At this temperature, the specimen was completely softened. With given stress, the length of the specimen increased, which was shown by the increase of strain. Then the temperature dropped to 50 °C, where the tension was released, which leads to resilience. Based on the value of strain, the fix ratio (R_f) from the original shape (shape 0) to the first shape (shape I) can be calculated, and it is 76%. At 50 °C, another stress is applied to the specimen, which lead to further elongation, and this is referred to as the second shape (shape II). Shape II is fixed at 0 °C, which yields R_f(I–II) = 89%. The shape fixing can be directly observed in Fig. 8 (the first three pictures). The shape

recovery is shown in the last two pictures of Fig. 8, and the recovery ratios, R_r(II–I) and R_r(I–0), are 79% and 93%, respectively.

The durability of the shape memory effect for the materials was investigated for PU and all PU/PMMA composites. A dual-shape memory cycle was repeated for each of the samples. The deformation temperature was set to 60 °C. The R_f and R_r values of the four cycles are shown in Table 2. With increases of the weight ratio of PMMA in the composites, both R_f and R_r increased substantially. For each specimen, both R_f and R_r decrease with the number of rounds. The PU/PMMA composites with low PMMA content behave very similarly to pure PU, which may be consistent with the results in the mechanical test. After the fourth round of testing, a high fix ratio remained for the composite with a weight ratio of 2 : 1; however, the recovery ratio reduced gradually, which could be caused by the break of the physical net points in the materials.

4 Conclusion

In this study, we used reaction-induced phase separation to synthesize PU/PMMA composites by adjusting the ratio between the two components. We found that, by changing the volume ratio of PU/PMMA, the composite showed microscopic phase separation. The microscopic phase separation visible in the SEM images manifested as a sea-island structure and was also quantitively described by the parameter, DPS. DPS increases with the volume ratio of PU/PMMA. When the volume ratio of PU/PMMA equals 2 : 1, the composite shows the highest DPS. Due to the microscopic phase separation, the mechanical properties also increased, which resulted in TSME. This indicates that TSME may be achieved by microscopic phase separation synthesized using reaction-induced phase separation. Due to the good biological compatibility of PU, the polymer composite may have potential applications as a biomedical material.

Acknowledgements

We thank financial supports from the Thousand Talents Program for Young Outstanding Scientists.

References

1 Y. Wu, J. Hu, C. Zhang, J. Han, Y. Wang and B. Kumar, *J. Mater. Chem. A*, 2015, **3**, 97–100.
2 Y. Li, H. Chen, D. Liu, W. Wang, Y. Liu and S. Zhou, *ACS Appl. Mater. Interfaces*, 2015, **7**, 12988–12999.
3 Q. Song, H. Chen, S. Zhou, K. Zhao, B. Wang and P. Hu, *Polym. Chem.*, 2016, **7**, 1739–1746.
4 N. Zheng, Z. Fang, W. Zou, Q. Zhao and T. Xie, *Angew. Chem., Int. Ed.*, 2016, **55**, 11421–11425.
5 P. T. Mather, X. Luo and I. A. Rousseau, *Annu. Rev. Mater. Res.*, 2009, **39**, 445–471.
6 T. Xie, *Polymer*, 2011, **52**, 4985–5000.
7 D. Ratna and J. Karger-Kocsis, *J. Mater. Sci.*, 2008, **43**, 254–269.
8 T. Gong, W. Li, H. Chen, L. Wang, S. Shao and S. Zhou, *Acta Biomater.*, 2012, **8**, 1248–1259.
9 H. Lu, W. Huang and Y. Yao, *Pigm. Resin Technol.*, 2013, **42**, 237–246.
10 K. K. Julich-Gruner, C. Löwenberg, A. T. Neffe, M. Behl and A. Lendlein, *Macromol. Chem. Phys.*, 2013, **214**, 527–536.
11 J. Hu, C. Zhang, X. Li, J. Han and F. Ji, *Polym. Chem.*, 2017, **8**, 260–271.
12 S. Chen, J. Hu, H. Zhuo, C. Yuen and L. Chan, *Polymer*, 2010, **51**, 240–248.
13 D. L. Safranski, J. M. Boothby, C. N. Kelly, K. Beatty, N. Lakhera, C. P. Frick, A. Lin, R. E. Guldberg and J. C. Griffis, *J. Mech. Behav. Biomed. Mater.*, 2016, **62**, 545–555.
14 X. Yang, L. Wang, W. Wang, H. Chen, G. Yang and S. Zhou, *ACS Appl. Mater. Interfaces*, 2014, **6**, 6545–6554.
15 X. Fan, B. H. Tan, Z. Li and X. J. Loh, *ACS Sustainable Chem. Eng.*, 2016, **4**(10), 5268–5276.
16 H. Zhang, H. Wang, W. Zhong and Q. Du, *Polymer*, 2009, **50**, 1596–1601.
17 S. Farzaneh, J. Fitoussi, A. Lucas, M. Bocquet and A. Tcharkhtchi, *J. Appl. Polym. Sci.*, 2013, **128**, 3240–3249.
18 N. Ahmed, A. Kausar and B. Muhammad, *Polym.-Plast. Technol. Eng.*, 2015, **54**, 1410–1423.
19 A. Cohades, E. Manfredi, C. J. Plummer and V. Michaud, *Eur. Polym. J.*, 2016, **81**, 114–128.
20 T. Xie, X. Xiao and Y.-T. Cheng, *Macromol. Rapid Commun.*, 2009, **30**, 1823–1827.
21 A. H. Torbati, H. B. Nejad, M. Ponce, J. P. Sutton and P. T. Mather, *Soft Matter*, 2014, **10**, 3112–3121.
22 Y. Zhang, X. Jiang, R. Wu and W. Wang, *J. Appl. Polym. Sci.*, 2016, **133**, 43534.
23 S. C. Glotzer, E. A. Di Marzio and M. Muthukumar, *Phys. Rev. Lett.*, 1995, **74**, 2034.
24 W. Wang and S. A. Sande, *Polym. J.*, 2015, **47**, 302–310.
25 Z. Wang, Q. Ran, R. Zhu and Y. Gu, *Phys. Chem. Chem. Phys.*, 2014, **16**, 5326–5332.
26 X. Li, X. Luo and Y. Gu, *Phys. Chem. Chem. Phys.*, 2015, **17**, 19255–19260.
27 W. Li, X. Jiang, R. Wu and W. Wang, *Polym. J.*, 2017, **49**, 263–271.
28 M. M. Coleman, D. J. Skrovanek, J. Hu and P. C. Painter, *Macromolecules*, 1988, **21**, 59–65.
29 C. Zhang, J. Hu, X. Li, Y. Wu and J. Han, *J. Phys. Chem. A*, 2014, **118**, 12241–12255.
30 L. Zhang, S. S. Shams, Y. Wei, X. Liu, S. Ma, R. Zhang and J. Zhu, *J. Mater. Chem. A*, 2014, **2**, 20010–20016.
31 L. Bistričić, G. Baranović, M. Leskovac and E. G. Bajsić, *Eur. Polym. J.*, 2010, **46**, 1975–1987.
32 T. Xie, *Nature*, 2010, **464**, 267–270.
33 B. Johnsen, A. Kinloch and A. Taylor, *Polymer*, 2005, **46**, 7352–7369.